Fault-Tolerant Tasking and Guidance of an Airborne Location Sensor Network

N. Eva Wu, Yan Guo, Kun Huang, Matthew C. Ruschmann, and Mark L. Fowler

Abstract: This paper is concerned with tasking and guidance of networked airborne sensors to achieve fault-tolerant sensing. The sensors are coordinated to locate hostile transmitters by intercepting and processing their signals. Faults occur when some sensor-carrying vehicles engaged in target location missions are lost. Faults effectively change the network architecture and therefore degrade the network performance. The first objective of the paper is to optimally allocate a finite number of sensors to targets to maximize the network life and availability. To that end allocation policies are solved from relevant Markov decision problems. The sensors allocated to a target must continue to adjust their trajectories until the estimate of the target location reaches a prescribed accuracy. The second objective of the paper is to establish a criterion for vehicle guidance for which fault-tolerant sensing is achieved by incorporating the knowledge of vehicle loss probability, and by allowing network reconfiguration in the event of loss of vehicles. Superior sensing performance in terms of location accuracy is demonstrated under the established criterion.

Keywords: Emitter location, fault-tolerant system, Markov decision problem, resource allocation, sensor network, trajectory generation.

1. INTRODUCTION

1.1. Objectives

Sensing principles are used in this paper as the basis for tasking networked airborne sensors and for deriving guidance criteria needed to coordinate multiple sensor-carrying vehicles that perform data acquisition for emitter location. The paper focuses on enhancing the network sensing performance in the face of loss of sensors. The resulting network is said to be fault-tolerant, which is made possible by the mobility and a multiplicity of the sensing nodes in the network.

Fault-tolerant tasking is achieved by implementing operation policies optimized for network availability. Fault-tolerant guidance is achieved by incorporating the likelihood of vehicle loss into generating vehicle trajectories, and by allowing network reconfiguration upon loss of vehicles.

Manuscript received September 15, 2007; accepted April 21, 2008. Recommended by Guest Editors Marcel Staroswiecki and Bin Jiang. This work was supported by the US Air Force Office of Scientific Research under Grants FA9550-06-0456 and FA9550-06-1-0249 along with the US Air Force Research Laboratory under Contract FA8750-07-1-0172.

N. Eva Wu, Yan Guo, Kun Huang, Matthew C. Ruschmann, and Mark L. Fowler are with the Department of Electrical and Computer Engineering, Binghamton University, Binghamton, NY 13902-6000, U.S.A. (e-mails: {evawu, yan.guo, kun.huang, matthew.ruschmann, mfowler}@binghamton.edu).

1.2. Related work

Discussion on two aspects of source location problems – target assignment, and guidance and control of multiple agents – has recently emerged in the controls literature [1,2]. The overall goal has been timely completion of sensing missions, such as search and surveillance, while avoiding conflicts, such as obstacles and collisions.

Location methods referred to in this body of literature, however, are mostly visual. The few that involve radio frequency sensors employ relatively simple and inaccurate sensing mechanisms, such as bearing only measurements [21], and signal strength measurements [17]. The latter reference describes a pursuit evasion game, where mobile agents are to chase and capture multiple moving targets in a minimum amount of time, and a network of stationary sensors serves to help enhance the target observability in the game.

Precision location of microwave transmitters is a mature technology [18]. With unmanned aerial vehicles (UAVs) replacing stationary sensor networks and manned vehicles, significant improvements can be expected in both speed and accuracy of sensing through guidance and control of the sensors. Networking in a hostile environment, however, poses special challenges. Data exchange inherent to a networked operation and prolonged mission time due to poor execution expose the otherwise passive location sensors, thus increase the likelihood of the

vehicles being destroyed.

The new development in this paper will be illustrated through passive sensing of microwave emitters with airborne sensors. In this case, each sensor-pair makes measurements on time difference of arrival (TDOA) and frequency difference of arrival (FDOA) of signals from stationary targets. The application of the TDOA/FDOA location technology to non-stationary emitters can be found in [10].

The approach to tasking taken in this paper at the abstract level resembles that described in [22] where a very different application field is considered.

1.3. Problem description via a simple example

This paper considers both tasking and vehicle guidance of a small scale airborne location sensor network. Examine a situation where the motion of two vehicles and a target lie within a plane, as illustrated in Fig. 1. Let us assume that the two vehicles are equipped to acquire both the time difference of arrival and the frequency difference of arrival of the target's signal. The sensors are mounted on the vehicles, and thus are subject to the same speed and curvature constraints as that of the vehicles. The sensors are passive nodes when acquiring data from the target, but become active (transmitters) when exchanging data between them in order to provide a location estimate.

It can be seen from Fig. 1 that, in a 2-dimensional setting[1], at least two vehicles are needed, making both a TDOA measurement and an FDOA measurement, to locate the target. A noiseless measurement of time difference of arrival by a pair of sensors on the two vehicles is given by

$$s_T = \frac{1}{c}[\sqrt{(x_2 - x_e)^2 + (y_2 - y_e)^2} - \sqrt{(x_1 - x_e)^2 + (y_1 - y_e)^2}], \quad (1)$$

and a noiseless measurement of frequency difference of arrival by the same pair of sensors is given by

$$s_F = \frac{f_e}{c}[\frac{(x_2 - x_e)u_2 + (y_2 - y_e)v_2}{\sqrt{(x_2 - x_e)^2 + (y_2 - y_e)^2}} - \frac{(x_1 - x_e)u_1 + (y_1 - y_e)v_1}{\sqrt{(x_1 - x_e)^2 + (y_1 - y_e)^2}}], \quad (2)$$

where (x_e, y_e) is the transmitter location to be estimated, (x_1, y_1) and (x_2, y_2) are the positions of the two vehicles, respectively, (u_1, v_1) and (u_2, v_2) are the velocities of the vehicles, f_e is the carrier

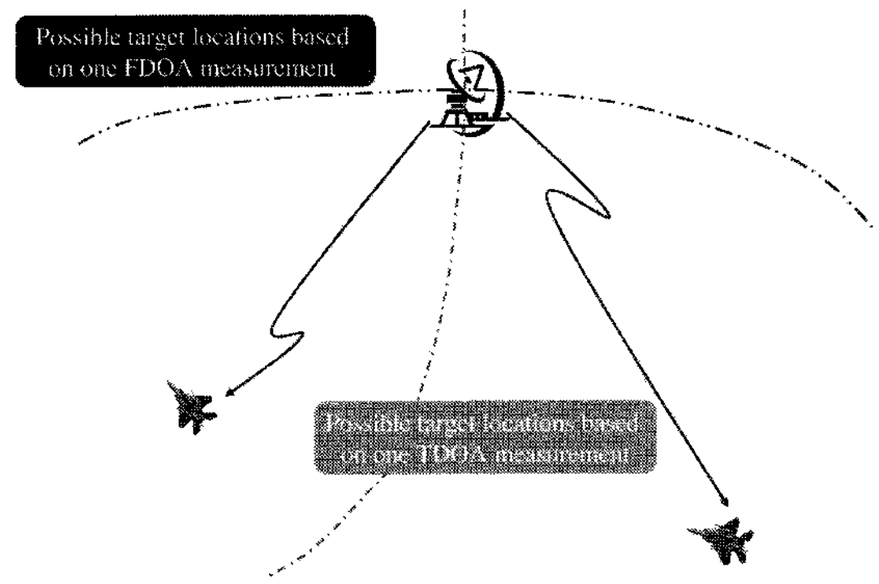

Fig. 1. Emitter location using a TDOA measurement and an FDOA measurement by two sensors.

frequency of the transmitted signal, and c is the speed of light.

Equations (1) and (2) clearly show the dependence of measurements on sensor *states* (x_i, y_i, u_i, v_i), $i = 1, 2$ which are non-stationary. Since the measurements are always noisy [20], multiple measurements are needed for an accurate location estimation of the emitter. Such measurements can be distributed temporally along the trajectories of motion of a pair of sensors, or spatially over multiple pairs of sensors, or both. Measurements made by multiple pairs of sensors, which form a network, offer greater degree of fault-tolerance, and greater potential for improved speed and accuracy in target location.

In this paper, a tasking problem refers to that of allocating a finite number of sensor pairs to randomly emerging targets to maximize the network availability. A tasking policy that is too greedy tends to exhaust resources before the arrival of unanticipated targets, whereas a tasking policy that is too conservative tends to lengthen the exposure of the sensor carrying vehicles. Optimal policies are sought as the solutions of Markov decision problems.

A guidance problem in this paper refers to that of establishing a criterion and deriving a set of desired vehicle trajectories under the criterion that the airborne sensors are expected to follow to expedite the target location estimation to a required accuracy. It will become clear that the quality of acquired data by the airborne sensors depends highly on both the network architecture which is determined by the number of sensor-pairs, and the *states* of all participating sensors relative to the target and to one another. A guidance principle is established by seeking the minimum of a scalar field weighted by the probabilities of vehicle losses to adjust the states of the sensors.

1.4. Organization of the paper

The paper is organized as follows. Section 2 discusses tasking sensor-pairs to targets for a small scale sensor network. The subsections cover modeling,

[1] In 3-d, at least 2 pairs of sensors are needed. Most academic treatments of location problems are limited to 2-d that is able to largely capture the problem essence.

policy design, and performance analysis for the location sensor network. Tasking is treated as a server allocation problem of a queuing network. Section 3 discusses fault-tolerant guidance of the vehicles allocated to a target. The subsections institutes a guidance criterion, explains the measures taken to achieve fault-tolerance, and presents the results of fault-tolerant guidance under the guidance criterion. Section 4 concludes the paper.

2. FAULT-TOLERANT TASKING

An optimized tasking is one that maximizes the expected life of the network where the lost airborne sensors cannot be replenished, or one that maximizes the expected steady-state availability of the network where the lost sensors can be replenished. In this study fault-tolerance refers to the network's tolerance to vehicle loss.

2.1. A queuing network model for tasking

Fig. 2 is a queuing network model of a six-sensor, finite target population tasking process, where each server represents a pair of sensors capable of independently locating a target to a certain accuracy in the absence of other pairs, and a customer is a randomly emerging target.

Each customer residing in the queue or in a server is regarded as a detected target which is to be or being served by one or more servers (sensor-pairs). Service is complete as soon as the target location is determined to a required accuracy. The target is then considered removed. A sensor-pair allocated to a target is tied to the target until its service is complete, or the life of the sensor-pair is terminated, whichever comes first. The three delay elements of average delay $1/\lambda$ imply that target population is limited by three at any given time. A new target is generated or replenished at a delay element with rate λ upon the service completion (removal) of a target at one or multiple servers.

A supervisory control policy determines whether to allocate one, two, or three pairs of sensors to each reported target, with a corresponding mean service time of $1/\mu_1, (\geq) 1/\mu_2, (\geq) 1/\mu_3$, respectively, where μ_i denotes the service rate of committing i pairs of sensors to a target. Given the sensing mechanism, the mean service time by a single pair of sensors is in the range of seconds to tens of seconds, dominated by the time required to adjust sensor positions and velocities for continued data collection needed for target location of a required accuracy. Each sensor-pair has a mean lifetime $1/\nu_0 \geq 1/\nu_1 \geq 1/\nu_2 \geq 1/\nu_3$, depending on the threat level quantified by the number of targets present as indexed by the subscript. $1/\nu_0$ is the mean server life representing the expected natural endurance

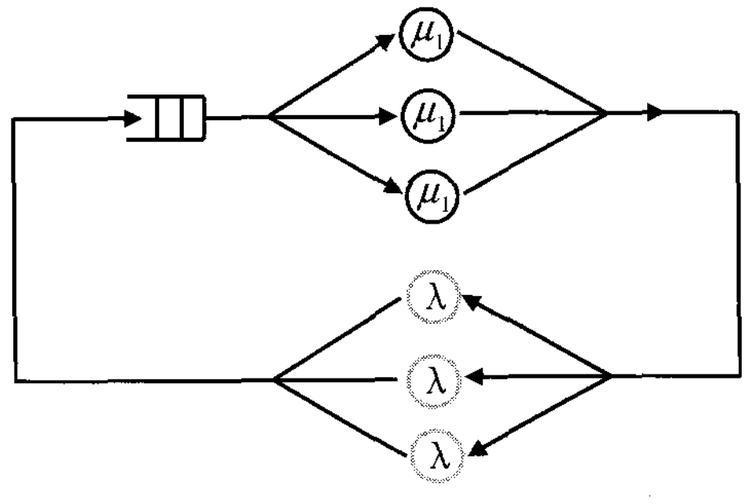

(a) One sensor-pair/target allocation.

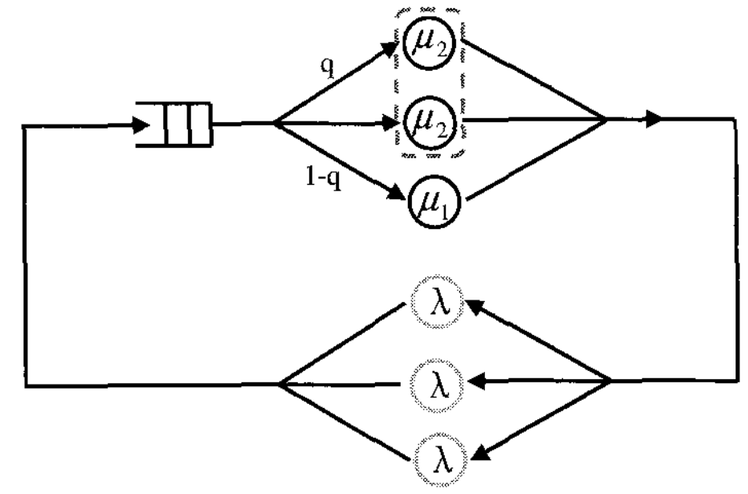

(b) Two sensor-pair/target allocation.

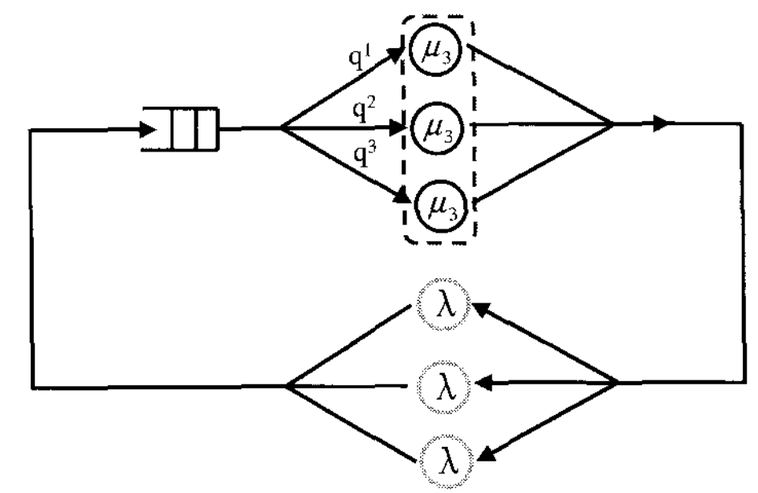

(c) Three sensor-pair/target allocation.

Fig. 2. A queuing network model of a three sensor-pair, finite target population airborne sensor network.

of a vehicle, which is "often an hour or so at best" [19]. It also reflects sensor lives affected by undetected targets. The network is said to have expired when there is no longer a single surviving sensor-pair.

The tasking process model is built in this study with the premise that event life distributions have been established for the process of target arrival $(\exp(\lambda) \equiv 1 - e^{-\lambda t})$, the process of target location $(\exp(\mu_i))$ with i pairs of sensors, the process of loss of a sensor-pair $(\exp(\nu_j))$, under threat level j, and the process of sensor replenishment $(\exp(\omega))$ when new sensor carrying vehicles are supplied for an expired network. Since all event lives are assumed to be exponentially distributed, the database unit can be conveniently modeled as a Markov chain specified by a state space $\mathcal{X}$, an initial state probability mass

function (pmf) $\pi_x(0)$, and a set of state transition rates λ, μ_i, ν_i, and ω.

A state name is coded with a 4-digit number indicative of the number of targets present and the network configuration. A valid state representation is given by QS, where queue length $Q \in \{0,1,2,3\}$, and server state $S=(i,j,k)$, with $i \in \{0,1,2,3,4\}$, and $j \in \{0,1,2,3,4,5\}$, and $k \in \{0,1,3,4,5\}$. A server state "0", represented by the value of i, or j, or k, indicates an idle sensor-pair, a "1" indicates that a target is being located by one server (or one sensor-pair), a "2" and a "3" indicate that a target's being located by two and three cooperating servers, respectively, a "4" indicates a lost server, and a "5" indicates that the lost server has been tied to another server in serving a target. The expired network requires 4 distinct states to memorize the possible number of targets present at the time of network expiration. Note that this state specification has assumed homogeneous sensor-pairs and homogeneous targets, and has made use of the symmetry which results in 37 states. A set of alternative state names are assigned from $\mathcal{X}=\{1,2,...,37\}$ with 0000 mapped to $x=1$ and the network expiration states mapped to $x=34,35,36,$ and 37.

Events that trigger the transitions and the corresponding transition rates are given as follows. An emerging target enters with rate $(3-Q)\times\lambda$. A target is located by one sensor-pair with rate μ_1, and $i(>1)$ cooperative sensor-pairs with rate μ_i. In the latter case, the i servers are configured as a single hyper-exponential server with i parallel stages [5]. An arriving target enters any one of the servers with probability $1/i$, which has a service time distribution $\exp(\mu_i)$. When service is completed, the target is removed, while no new target can enter service when the hyper-exponential server is busy. The service time distribution of a hyper-exponential server is

$$F_i(t)=\sum_{j=1}^{i}\frac{1}{i}(1-e^{-\mu_i t})=1-e^{-\mu_i t}, \quad (3)$$

as a result of assuming homogeneity of both the servers and the targets. Loss of a sensor-pair occurs at rate $m\nu_0$ when the network is idle with m remaining sensor-pairs, $m\nu_1$ when one target emerges, and $m\nu_i$ when $i(>1)$ targets emerge. Replenishment process begins at the network expiration with rate ω. If one of the sensor-pairs is lost while locating a target with other sensor-pairs, the surviving sensor-pairs continue to locate the target at the same rate. This is a simple way to memorize the service already being provided without resorting to a more complex model.

Let $X \in \mathcal{X}$ denote the random state variable at time t. The set of state transition functions is given by

$$p_{i,j}(t) \equiv P[X(t)=j \mid X(0)=i], \quad i,j=1,2,...,37. \quad (4)$$

The continuous-time Markov chain can be solved from the forward Chapman-Kolmogorov equation [5,11]

$$\dot{P}(t)=P(t)Q(u(x)), \quad P(0)=I, \quad P(t)=[p_{i,j}(t)], \quad (5)$$

and $Q(u(x))$ is called an infinitesimal generator or a rate transition matrix whose $(i,j)^{th}$ entry is given by the rate associated with the transition from current state i to next state j. Fig. 3 summarizes information contained in transition rate matrix $Q(u(x))$. Control variable $u(x)$ will be discussed shortly. State probability mass function at time t

$$\pi(t)=[\pi_1(t)\ \pi_2(t)\cdots\pi_{37}(t)], \quad t\geq 0 \quad (6)$$

can be solved from

$$\dot{\pi}(t)=\pi(t)Q(u(x)), \quad \text{given } \pi(t=0). \quad (7)$$

A Markov chain for the tasking process of Fig. 2 has been established so far. Since transition rate matrix Q is dependent on control actions, the state transition functions $p_{i,j}(t)$ are being controlled, and so are the state probabilities.

2.2. Design of supervisory control policy

Several possible supervisory control policies associated with tasking are examined. An aggressive policy allocates as many available sensor-pairs to as many targets present; A greedy policy allocates all available sensor-pairs to one target at a time; A conservative policy always allocates only one sensor-pair to every target present to reserve assets in anticipation of new targets[2]. In addition, four optimal policies are attempted to minimize the cost of sensor loss rate, threat level, unattended targets, and time needed to replenish upon network expiration, respectively.

The optimal policies are obtained by solving Markov decision problems of appropriate penalty functions. A discrete-time Markov chain model suitable for this purpose can be derived under each cost criterion by the application of a uniformization procedure [12]

$$\pi(t_{k+1})=\pi(t_k)[I+\frac{1}{\rho}Q(u(x_k))], \quad (8)$$

[2] Again this assumes a 2-dimensional setting.

x	Coded x				Arrivals						Completions						Losses & Replenishements					
	Q	S1	S2	S3	x'	Rate	x'	Rate	x'	Rate	x'	Rate	x'	Rate	x'	Rate	x'	Rate	x'	Rate	x'	Rate
1	0	0	0	0	4	$3*\lambda*u1$	7	$3*\lambda*u2$	9	$3*\lambda*u3$	x	x	x	x	x	x	2	$3*v_0$	x	x	x	x
2	0	4	0	0	5	$3*\lambda*u1$	8	$3*\lambda*u2$	x	x	x	x	x	x	x	x	3	$2*v_0$	x	x	x	x
3	0	4	4	0	6	$3*\lambda$	x	x	x	x	x	x	x	x	x	x	34	v_0	x	x	x	x
4	1	1	0	0	10	$2*\lambda*u1$	13	$2*\lambda*u2$	x	x	1	μ_1	x	x	x	x	5	$3*v_1$	x	x	x	x
5	1	1	4	0	11	$2*\lambda$	x	x	x	x	2	μ_1	x	x	x	x	6	$2*v_1$	x	x	x	x
6	1	1	4	4	12	$2*\lambda$	x	x	x	x	3	μ_1	x	x	x	x	35	v_1	x	x	x	x
7	1	2	2	0	13	$2*\lambda$	x	x	x	x	1	μ_2	x	x	x	x	22	$2*v_1*u1$	8	v_1*u2	x	x
8	1	2	2	4	14	$2*\lambda$	x	x	x	x	2	μ_2	x	x	x	x	23	$2*v_1$	x	x	x	x
9	1	3	3	3	15	$2*\lambda$	x	x	x	x	1	μ_3	x	x	x	x	26	$3*v_1$	x	x	x	x
10	2	1	1	0	16	λ	x	x	x	x	4	μ_1	x	x	x	x	11	$3*v_2$	x	x	x	x
11	2	1	1	4	17	λ	x	x	x	x	5	μ_1	x	x	x	x	12	$2*v_2$	x	x	x	x
12	2	1	4	4	18	λ	x	x	x	x	6	μ_1	x	x	x	x	36	v_2	x	x	x	x
13	2	2	2	1	19	λ	x	x	x	x	7	μ_1*u1	4	μ_2*u2	x	x	24	$2*v_2*u1$	14	v_2*u2	x	x
14	2	2	2	4	20	λ	x	x	x	x	5	μ_2*u1	8	μ_2*u2	x	x	30	$2*v_2$	x	x	x	x
15	2	3	3	3	21	λ	x	x	x	x	4	μ_3*u1	7	μ_3*u2	9	μ_3*u3	28	$3*v_2$	x	x	x	x
16	3	1	1	1	x	x	x	x	x	x	10	μ_1	x	x	x	x	17	$3*v_3$	x	x	x	x
17	3	1	1	4	x	x	x	x	x	x	11	μ_1	x	x	x	x	18	$2*v_3$	x	x	x	x
18	3	1	4	4	x	x	x	x	x	x	12	μ_1	x	x	x	x	37	v_3	x	x	x	x
19	3	2	2	1	x	x	x	x	x	x	10	μ_2*u1	13	μ_2*u2	x	x	25	$2*v_3*u1$	20	v_3*u2	x	x
20	3	2	2	4	x	x	x	x	x	x	11	μ_2*u1	14	μ_2*u2	x	x	33	$2*v_3$	x	x	x	x
21	3	3	3	3	x	x	x	x	x	x	10	μ_3*u1	13	μ_3*u2	15	μ_3*u3	31	$3*v_3$	x	x	x	x
22	1	2	5	0	24	$2*\lambda$	x	x	x	x	2	μ_2	x	x	x	x	6	v_1*u1	23	v_1*u2	x	x
23	1	2	5	4	30	$2*\lambda$	x	x	x	x	3	μ_2	x	x	x	x	35	v_1	x	x	x	x
24	2	2	5	1	25	λ	x	x	x	x	22	μ_1*u1	5	μ_2*u2	x	x	12	v_2*u1	30	v_2*u2	x	x
25	3	2	5	1	x	x	x	x	x	x	24	μ_1*u1	11	μ_2*u2	x	x	18	v_3*u1	33	v_3*u2	x	x
26	1	3	3	5	28	$2*\lambda$	x	x	x	x	2	μ_3	x	x	x	x	27	$2*v_1$	x	x	x	x
27	1	3	5	5	29	$2*\lambda$	x	x	x	x	3	μ_3	x	x	x	x	35	v_1	x	x	x	x
28	2	3	3	5	31	λ	x	x	x	x	5	μ_3*u1	8	μ_3*u2	x	x	29	$2*v_2$	x	x	x	x
29	2	3	5	5	32	λ	x	x	x	x	6	μ_3	x	x	x	x	36	v_2	x	x	x	x
30	2	2	5	4	33	λ	x	x	x	x	6	μ_2	x	x	x	x	36	v_2	x	x	x	x
31	3	3	3	5	x	x	x	x	x	x	11	μ_3*u1	14	μ_3*u2	x	x	32	$2*v_3$	x	x	x	x
32	3	3	5	5	x	x	x	x	x	x	12	μ_3	x	x	x	x	37	v_3	x	x	x	x
33	3	2	5	4	x	x	x	x	x	x	12	μ_2	x	x	x	x	37	v_3	x	x	x	x
34	0	4	4	4	x	x	x	x	x	x	x	x	x	x	x	x	1	w	x	x	x	x
35	1	4	4	4	x	x	x	x	x	x	x	x	x	x	x	x	4	$w*u1$	7	$w*u2$	9	$w*u3$
36	2	4	4	4	x	x	x	x	x	x	x	x	x	x	x	x	10	$w*u1$	13	$w*u2$	15	$w*u3$
37	3	4	4	4	x	x	x	x	x	x	x	x	x	x	x	x	16	$w*u1$	19	$w*u2$	21	$w*u3$

$u1=l_1$, $u2=l_2$, $u3=l_3$, x: current state, x': next state

Fig. 3. Transitions and transition rates of the tasking process.

where the uniform rate ρ is greater than any total outgoing transition rates at any states of the original continuous-time Markov chain (7).

Each Markov decision problem considered in this paper assumes that a cost, denoted by $C(i,u)$, is incurred at every state transition, where i is the state entered and u is a control action selected from a set of admissible actions [3,5]. A solution amounts to determining a stationary policy $\pi = \{u(x_k), k = 0,1,\cdots\}$ that minimizes the following expected total discounted cost

$$V_\pi(x_0) = E_\pi \sum_{k=0}^{\infty} \alpha^k C(X_k, u_k), \tag{9}$$

where $0 < \alpha < 1$ is a discount factor, and $X_k \in \{1,2,\cdots,37\}$ denotes the random state variable at $t_k = k/\rho$ in the discrete time Markov chain. $C(X_k, u_k)$ in each of the four Markov decision problems takes the form of total number of lost sensor-pairs, ω^{-1} at the state of network expiration, v_i at the state where it is the server loss, and Q at the state where it is the queue length, respectively.

The control variable is defined as

$$u(x_k) = \begin{cases} 1, & \text{allocate one sensor – pair to a target being located;} \\ 2, & \text{allocate two sensor – pairs to a target being located;} \\ 3, & \text{allocate three sensor – pairs to a target being located.} \end{cases} \tag{10}$$

Note that the indicator functions in the table of Fig. 3

are defined as follows

$$I_i = \begin{cases} 1, & u = i \\ 0, & \text{otherwise} \end{cases}, \quad i = 1,2,3. \tag{11}$$

It is known [3,5] that under the condition $0 \le C(j,u) < \infty$ for all j and all u that belong to some finite admissible sets U_j, the minimum cost $V^*(i)$ satisfies the following optimality equation:

$$V(i) = \min_{u \in U_i} \left\{ C(i,u) + \alpha \sum_{j=1}^{37} p_{i,j} V(j) \right\}, u \in U_i, \tag{12}$$

where $i = 1,\ldots,37$ and $p_{i,j}$ is the $(i,j)^{th}$ entry of $I + \frac{1}{\rho} Q(u(x_k))$.

The solution to (12) can be obtained via linear programming [4]. In this case, the set of optimality equations is turned into a set of affine constraints on the set of optimization variables $\{V(i)\}$, and the problem can be formally stated as follows [3].

$$\text{Maximize}: \; V(1) + V(2) + \cdots + V(36) + V(37) \tag{13}$$

$$\text{Subject to}: \; V(i) \ge 0, \; i \in \mathcal{X} = \{1,\cdots,37\} \tag{14}$$

$$V(i) \le [C(i,u) + \alpha \sum_j p_{i,j} V(j)]|_u, \quad \forall u \in U_i, \; i \in \mathcal{X}. \tag{15}$$

In the tasking process considered, U_j is nonempty only at state $j = 1, 2, 4, 7, 13, 14, 15, 19, 20, 21, 22, 24, 25, 28, 31, 35, 36, 37$ (see Fig. 3). Therefore, (15) leads to 99 affine inequality constraints. This problem is readily solvable by *linprog* in MATLAB's Optimization Toolbox [15].

Fig. 4 shows an example of 4 stationary control policies depicted in terms of indicator functions, as

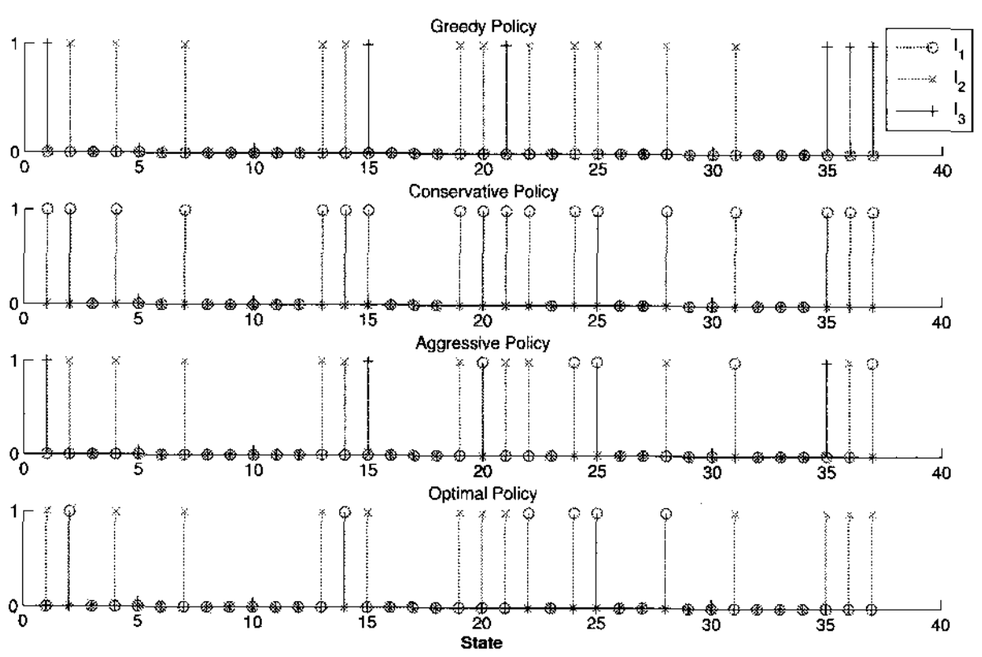

Fig. 4. Control policy indicators. red: one sever per target; green: two servers per target; blue: three servers per target.

defined in (11), of the state $x \in \mathcal{X}$. It can be seen that the optimal policy takes into consideration of anticipated targets more than the aggressive policy, but is much more aggressive in terms of use of resources than the conservative policy. Among the four optimal policies solved, only the policy derived under the least sensor loss is plotted (bottom), which will be shown shortly to outperform other three optimal policies in terms of both mean time to network expiration (MTTNE) and availability. The minimum queue length policy coincides with the greedy policy, as expected. The other two optimal policies make less aggressive use of resources than the least sensor loss policy shown. The least sensor loss policy will be called *the* optimal policy, or optimal policy 1 from this point on.

The control policies are robust with respect to the range of parameter variations that have been examined: $\nu_1 \in [0.001, 0.01]$ 1/sec, and $\lambda \in [0.001, 0.1]$ 1/sec. The optimal policy is calculated at $\alpha = 0.0792$. All optimal policies drift slightly toward more conservative actions (using fewer resources) as the discount factor α increases, which is consistent with the outcome of the longer term policy making. Because of the finite target population setup, the effect of increasing the target arrival rate is not fully reflective of the target traffic intensity. Simulations with *MATLAB SimEvents* [16] are being performed without limiting the target population.

2.3. Performance analysis

The seven policies developed in Section 2.2 are compared against one another with respect to two common measures of fault-tolerance: mean time to network expiration (MTTNE) and availability. These have been used in [22] in a similar fashion as performance measures of a database unit.

When no replenishment is provided, the network life eventually expires when all sensor-pairs are lost. This occurs when the network enters one of its absorbing states at 34, 35, 36, or 37. Decompose the state probability vector

$$\pi(t) = [\underbrace{\pi_\tau(t)}_{1\times 33} \; \underbrace{\pi_\alpha(t)}_{1\times 4}], \tag{16}$$

where vector $\pi_\tau(t)$ contains transient state probabilities, and $\pi_\alpha(t)$ contains absorbing state probabilities. Decomposing the rate transition matrix Q accordingly yields

$$Q = \begin{bmatrix} Q_{11} & Q_{12} \\ 0 & 0 \end{bmatrix}. \tag{17}$$

From (17), it can be determined that mean time to network expiration is given by

$$\text{MTTNE} = -\pi_\tau(0)Q_{11}^{-1}1_\tau,\ 1_\tau = [\underbrace{1\cdots1}_{1\times33}]^T. \tag{18}$$

Suppose as soon as the network expires, a replenishment process starts. Suppose with a rate ω the airborne sensors are replenished, and at the completion of the replenishment, the tasking process immediately resumes. In this case, the Markov chain (7) becomes irreducible, and a unique steady-state distribution exists [12]. The steady-state availability, which can be roughly thought of as the fraction of time the network has at least one surviving pair of sensors, is computed by

$$A_{net} = 1 - \pi_F(\infty), \tag{19}$$

where $\pi_F(\infty) = \pi_{34}(\infty) + \pi_{35}(\infty) + \pi_{36}(\infty) + \pi_{37}(\infty)$, the sum of state probabilities associated with network expiration, which can be determined by solving

$$\pi(\infty)Q = 0, \text{ and } \sum_{x=1}^{37}\pi_x(\infty) = 1. \tag{20}$$

A slightly different notion of availability is also examined, where the network is considered unavailable as long as some targets present are unattended. In this case, the network availability is given by

$$\begin{aligned} A_{tgt} = &\sum_{i=1}^{11}\pi_i(\infty) + \pi_{13}(\infty) + \pi_{16}(\infty) + \pi_{22}(\infty) \\ &+ \pi_{23}(\infty) + \pi_{24}(\infty) + \pi_{26}(\infty) + \pi_{27}(\infty). \end{aligned} \tag{21}$$

Mean time to network expiration is plotted in Fig. 5 against target arrival rate with two sets of sensor loss rates as parameters at $\alpha = 0.0792$. It shows that optimal policy compromises between being too

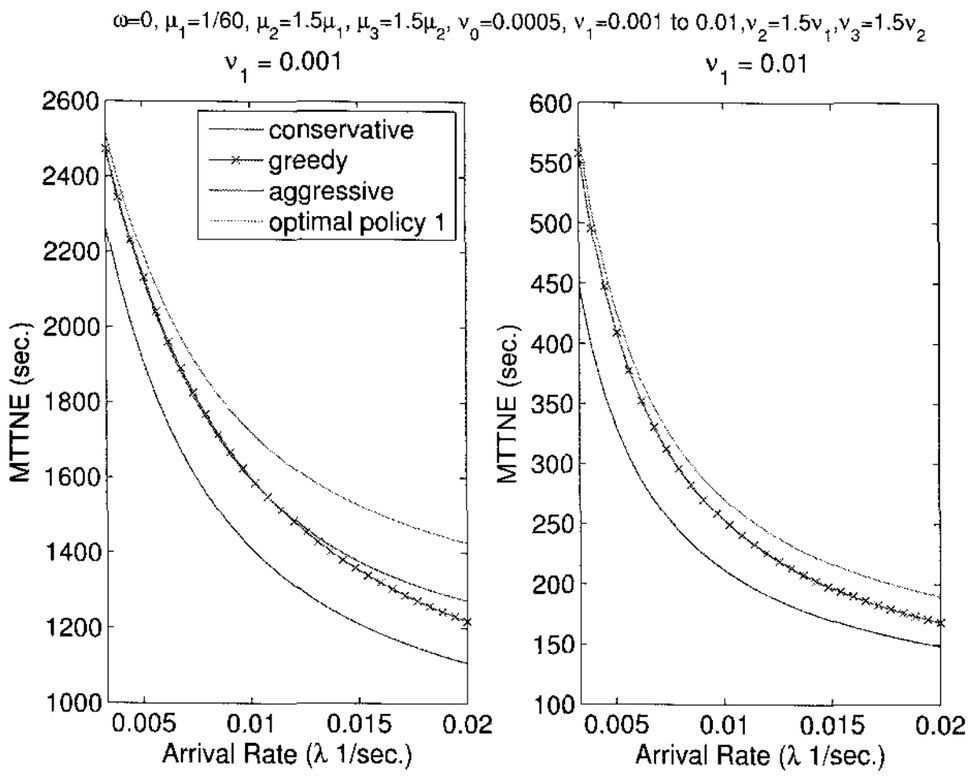

Fig. 5. Mean time to network expiration as a function of target arrival rate with two sets of sensor loss rates as parameters.

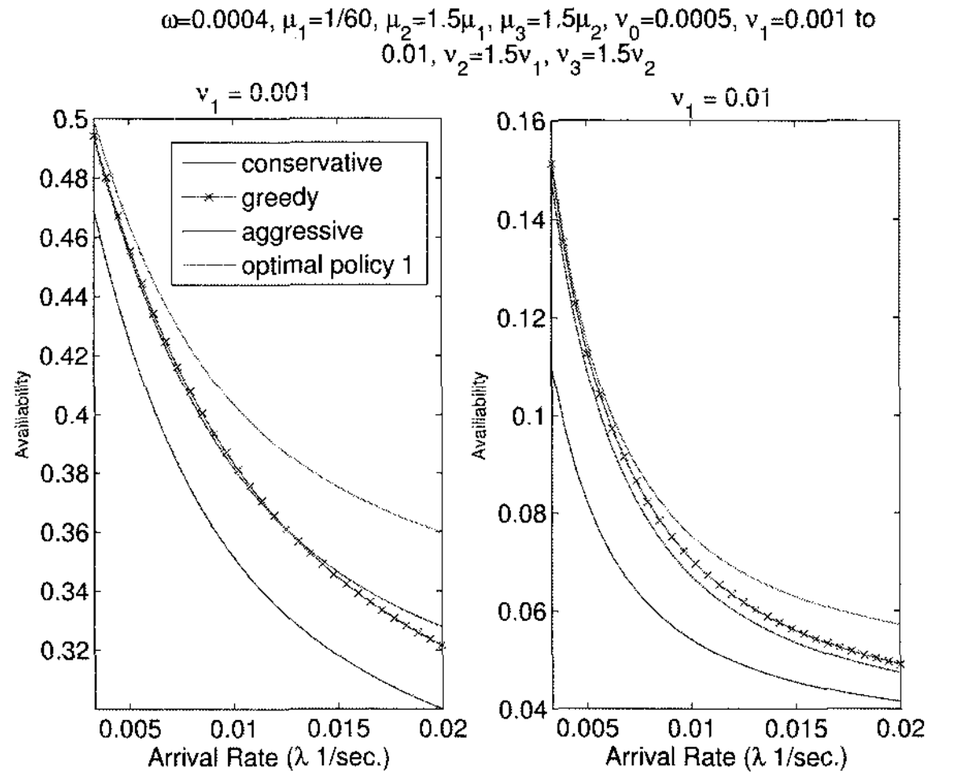

Fig. 6. Network availability with at least one surviving server.

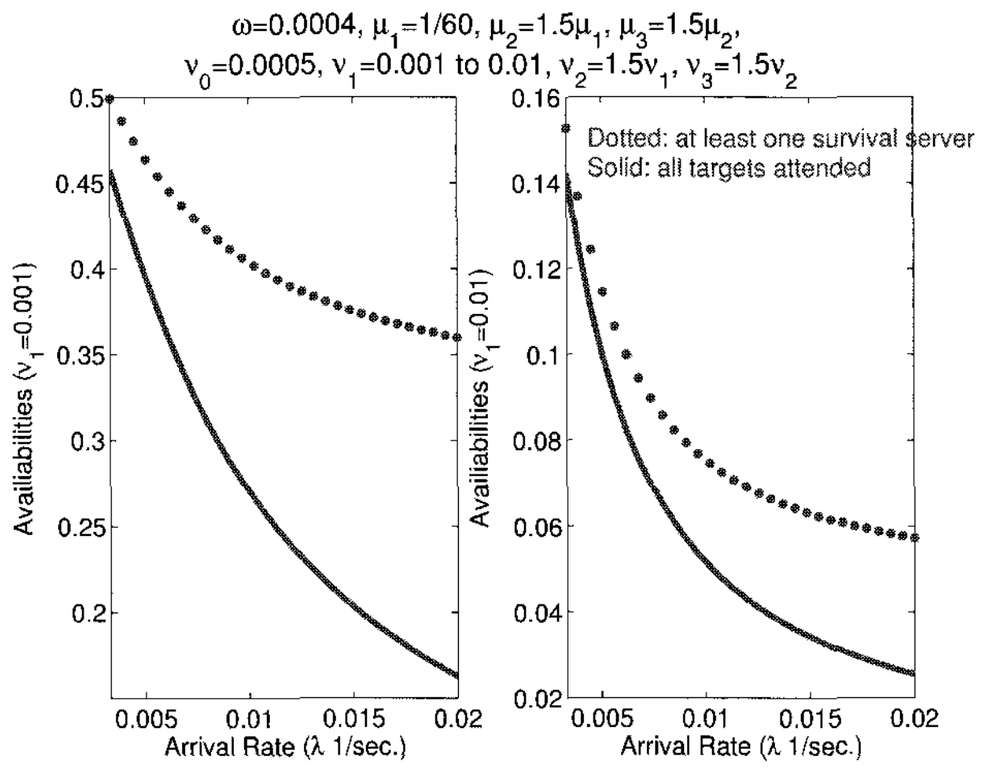

Fig. 7. Comparison between availability with at least one surviving server (dash) and availability with all targets being attended (solid).

greedy and too conservative, and enhances the network life consistently for all parameters values considered.

In Fig. 6, availability is plotted against target arrival rate with two sets of sensor loss rates as parameters at discount factor $\alpha = 0.0792$. The observations from the MTTNE apply in terms of the benefits the optimal policy offers. It is noted that the availability is rather low. This is because of the low replenishment rate used in the computation, which corresponds to an expected time of more than 40 minutes to reestablish the lost network.

It is expected that the network availability defined as the probability that all targets are attended is lower than the availability defined as the probability that there is at least one surviving server. On the other hand, the dependence of both notions of availability on the sensor loss rate and on the target arrival rate stays the same. Fig. 7 shows the plot of the two

availabilities against target arrival rate with two sets of sensor loss rates ν_i as parameters under the optimal policy.

Extensive simulations using [16] are being conducted to generate a more complete picture of the network performance in response to control policies for a larger size of networks. The results will be reported separately elsewhere.

3. FAULT-TOLERANT GUIDANCE

A certain number of pairs of sensors has now been allocated to each target present. The focus is now shifted to determining the rule of maneuvering a given set of sensors to best locate their assigned target. Microwave emitter location through TDOA/FDOA sensing using paired sensors is assumed. The restriction to the specific sensing mechanisms is important in that many critical issues and challenges raised in network performance are intimately tied to specific sensing methods.

This section starts with describing a sensing principle-based guidance criterion, and proceeds to presenting the results of fault-tolerant guidance under the criterion.

3.1. Sensing principle-based guidance criteria

Let $\mathbf{p}_e = (x_e, y_e)$ be the emitter location, and $\mathbf{z}_i \equiv (x_i, y_i, u_i, v_i)$ be the state of the i th sensor. Consider a set of $2N$ measurements collected by N pairs of sensors in the presence of additive errors

$$\mathbf{r} = \mathbf{g}(\mathbf{p}_e;\mathbf{z}) + \mathbf{n} = \begin{bmatrix} s_T^1(\mathbf{p}_e;\mathbf{z}_1,\mathbf{z}_2) \\ s_F^1(\mathbf{p}_e;\mathbf{z}_1,\mathbf{z}_2) \\ \vdots \\ s_T^N(\mathbf{p}_e;\mathbf{z}_{2N-1},\mathbf{z}_{2N}) \\ s_F^N(\mathbf{p}_e;\mathbf{z}_{2N-1},\mathbf{z}_{2N}) \end{bmatrix} + \begin{bmatrix} n_T^1 \\ n_F^1 \\ \vdots \\ n_T^N \\ n_F^N \end{bmatrix}, \tag{22}$$

where s_T^i and s_F^i are the TDOA and FDOA measurement models defined in (1) and (2), respectively, and $\mathbf{z} = (\mathbf{z}_1, \mathbf{z}_2, \cdots, \mathbf{z}_{2N})$ is the Cartesian product. By including a time index to $\mathbf{z}_i$, it is not difficult to extend the above expression to represent multiple measurements [20] by each sensor over time. Under a weighted least squares criterion with a $C_{2N\times 2N} > 0$

$$J(\mathbf{p}_e) = [\mathbf{r} - \mathbf{g}(\mathbf{p}_e;\mathbf{z})]^T C^{-1} [\mathbf{r} - \mathbf{g}(\mathbf{p}_e;\mathbf{z})], \tag{23}$$

the estimation error propagates according to

$$\hat{\mathbf{p}}_e^{k+1} - \hat{\mathbf{p}}_e^k = (G_k^T C^{-1} G_k)^{-1} G_k^T C^{-1} [\mathbf{r} - \mathbf{g}],$$

$$G_k(\hat{\mathbf{p}}_e^k;\mathbf{z}) \equiv \left.\frac{\partial \mathbf{g}(\mathbf{p}_e;\mathbf{z})}{\partial \mathbf{p}_e}\right|_{\mathbf{p}=\hat{\mathbf{p}}_e^k}. \tag{24}$$

The above is also known as the Gauss-Newton algorithm [7]. In general, algorithms that estimate emitter locations from noisy measurements are mature technologies [9], and will not be detailed in this paper. To simplify the notation, iteration index k is suppressed from this point on.

Estimator in (24) results in the linearized least-squares estimator when $\mathbf{g}(\mathbf{p}_e;\mathbf{z})$ in (23) is replaced by $G\mathbf{p}_e - G\hat{\mathbf{p}}_e + \mathbf{g}(\hat{\mathbf{p}}_e;\mathbf{z})$.

Minimizing the expected value of (23) leads to a maximum likelihood estimator, provided that $\mathbf{r}$ is random, obeying a Gaussian distribution with C as its covariance matrix[3]. In this case $\hat{\mathbf{p}}_e$ is Gaussian with covariance

$$\begin{aligned} P &\equiv E[(\hat{\mathbf{p}}_e - E(\hat{\mathbf{p}}_e))(\hat{\mathbf{p}}_e - E(\hat{\mathbf{p}}_e))^T] \\ &= [G^T(\hat{\mathbf{p}}_e;\mathbf{z}) C^{-1} G(\hat{\mathbf{p}}_e;\mathbf{z})]^{-1}. \end{aligned} \tag{25}$$

For a given $\kappa > 0$,

$$R_\kappa \equiv \{\mathbf{p} \mid (\mathbf{p} - E(\mathbf{p})^T P^{-1} (\mathbf{p} - E(\mathbf{p}) \le \kappa\} \tag{26}$$

defines an ellipsoid with semi-axis $\sqrt{\kappa\lambda_i}$, where λ_i is the i th largest eigenvalue of P. R_κ is called a concentration ellipsoid, and its volume $vol(R_\kappa)$ is often used to indicate the accuracy of an estimate for a specified value of probability [20]

$$Pr[\mathbf{p} \in R_\kappa] = \int_{R_\kappa} \frac{e^{-\frac{1}{2}(\mathbf{p}-E(\mathbf{p})^T P^{-1}(\mathbf{p}-E(\mathbf{p})}}{(2\pi)^n \sqrt{det(P)}} d\mathbf{p}. \tag{27}$$

In two dimensional and three dimensional cases [20], $Pr[\mathbf{p} \in R_\kappa]$ is given by $1 - e^{-\kappa/2}$, and $\frac{2}{\sqrt{\pi}} \cdot \int_0^{\sqrt{\kappa/2}} e^{-x^2} dx - \frac{\sqrt{2\kappa}}{\pi} e^{-\kappa/2}$, with volumes $vol(R_\kappa)$ given by $\pi\kappa\sqrt{det(P_{2\times 2})}$, and $\frac{4}{3}\pi\kappa^{3/2}\sqrt{det(P_{3\times 3})}$, respectively. $Pr[\mathbf{p} \in R_\kappa]$ is easily seen to be an increasing function of κ.

The expression in (25) reveals that gradient G defined in (24) can alter location accuracy because of the dependence of TDOA and FDOA measurements on sensor states $\mathbf{z}_i \equiv (x_i, y_i, u_i, v_i)$, and thus suggests the utility of $vol(R_\kappa)$ or $det(P)$ as a guidance

[3] The measurement error is in fact Gaussian asymptotically when the TDOA/FDOA estimates are afforded by a maximum likelihood estimator [13] from a large data set.

criterion. The latter is proportional to $vol^2(R_\kappa)$ for a given κ.

Denote by $A_i(\tau)$ for sensor i the set of states reachable by the airborne sensor within a specified amount of time τ from its current state $\mathbf{z}_i$ under some speed and thrust constraints. $A_i(\tau)$ is assumed available in this paper. Effort in characterization and calculation of such reachable sets is on going, and will be reported separately in the near future. The criterion by which a sensor state is selected within the reachable set to gain quality in data acquisition for target location is called a guidance criterion.

Based on an initial estimate[4] of a target location $\hat{\mathbf{p}}_e$, and the knowledge of measurement error covariance C, we seek to establish a guidance criterion for updating the states of all airborne sensors allocated to an already detected target to $\mathbf{z}_i^+$, reachable from their respective current states $\mathbf{z}_i, i=1,\cdots,2N$, to best fit the available estimate within a specified amount of time. Therefore, in the sensor state update problem, the roles of the known and the unknown between assumed transmitter location $\hat{\mathbf{p}}_e$, and predicted best sensor state $\mathbf{z}_i^+$ are reversed. The sensors are then guided to the updated states, from which new target data are acquired to update location estimate to $\hat{\mathbf{p}}_e^+$.

Consider Cartesian product $\mathbf{z}=(\mathbf{z}_1,\mathbf{z}_2,\cdots,\mathbf{z}_{2N})$, where $\mathbf{z}_i \in A_i$, and cylindrical extension [14] of reachable sets A_i, $i=1,\cdots,2N$, in the Cartesian product space. Let A_c be a convex subset of the extension. Then

$$\min_{\mathbf{z}^+\in A_c} V(\hat{\mathbf{p}}_e,\mathbf{z}^+) \equiv \min_{\mathbf{z}^+\in A_c} vol[R_\kappa(\hat{\mathbf{p}}_e,\mathbf{z}^+)] \tag{28}$$

is a meaningful guidance criterion, which minimizes the volume of the ellipsoid defined by R_κ that specifies the probability of hit for a fixed κ as seen in (27). It is noted that the above defined volume in fact is an area in the two dimensional setting of Fig. 1. From (23), the location estimation problem can be recast as

$$\min_{\hat{\mathbf{p}}_e^+} J(\hat{\mathbf{p}}_e^+) = \min_{\hat{\mathbf{p}}_e^+} [\mathbf{r}-\mathbf{g}(\hat{\mathbf{p}}_e^+,\mathbf{z})]^T C^{-1}[\mathbf{r}-\mathbf{g}(\hat{\mathbf{p}}_e^+,\mathbf{z})]. \tag{29}$$

Two related issues are being investigated. One is the rate of convergence to the best unbiased location estimate by iterating between (28) and (29). Another is the rate of sensor state update using guidance criterion (28). A brief description of our practice so far regarding the two issues, and some observations from simulations are provided.

Typically several thousand signal samples are collected after sensors' arrival at some $\mathbf{z}$ to update a location estimate to $\hat{\mathbf{p}}_e^+$ using (29). At the same time $\mathbf{z}^+$ is calculated using (28) based on the recent estimate $\hat{\mathbf{p}}_e^+$. The vehicles are then guided to $\mathbf{z}^+$ by applying the right thrusts (controls), and the process repeats. The process of updating on $\mathbf{z}$ terminates when a prescribed estimation accuracy is met, or when a prescribed time limit is reached.

The time interval specified in our simulations to drive the tasked airborne sensors from $\mathbf{z}$ to $\mathbf{z}^+$ is in the order of a few seconds. This interval reflects the attempt to balance among the size of each reachable set, which has an exponentially growing computational intensity as the time interval lengthens, the desire to locate the target in a timely manner, and time required to calculate $\mathbf{z}^+$. Optimizing the rate of sensor state updates under a guidance criterion is conceivably an extremely complex problem for which no formal solutions have been pursued so far.

Simulations of a four-sensor network have shown that iteration between (28) and (29) has sped up convergence. Fig. 8 compares the area of the 50% concentration ellipse, as defined in (26) and (27), calculated based on 50 independent location estimates with sensor state optimizations performed in 5 consecutive 10 second intervals, with that of the 50 estimates where the sensor velocities remain at their initial random values. Fig. 9 shows a sample set of trajectories generated by using the volume-based criterion for the four sensors.

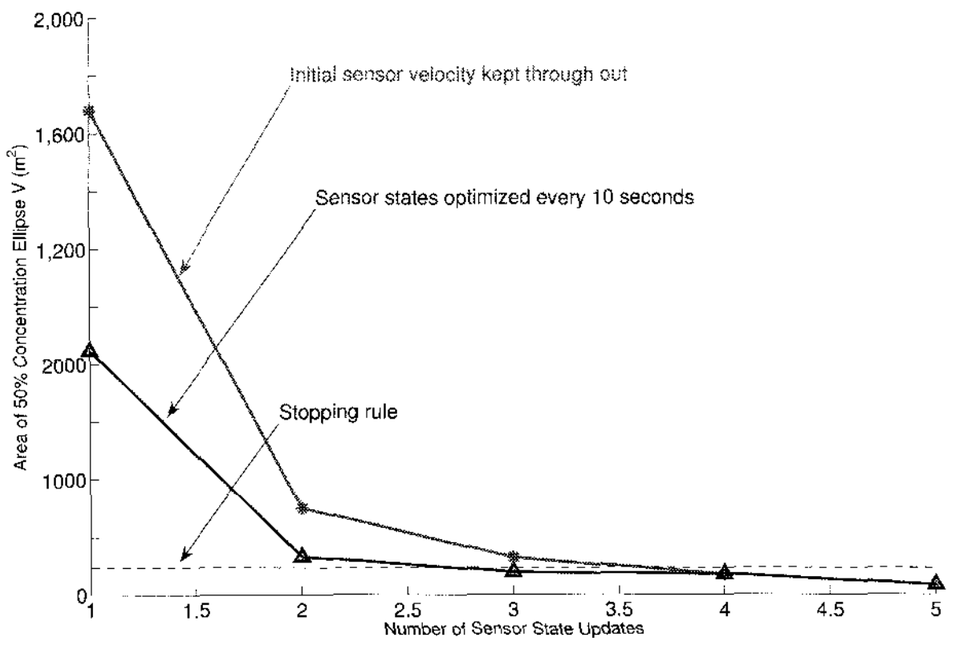

Fig. 8. Comparison of 50% concentration ellipses with (blue) and without (red) sensor state optimization based on 50 estimates at each update for each case.

[4] An initial estimate can come from previous activities of the current set of sensors, or another set of sensors, or as a cue from some other asset.

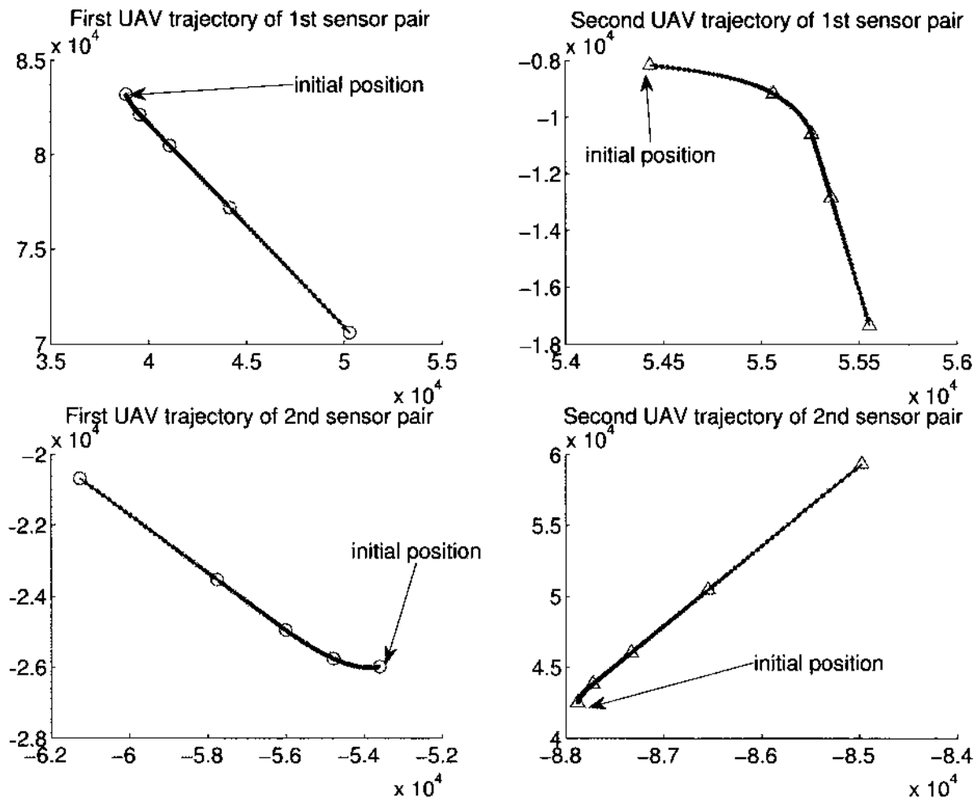

Fig. 9. Sample trajectories of a four sensor network calculated through 4 consecutive sensor state optimizations of 10 second interval for each update.

The conditions for the simulations are set as follows. The initial velocities of the sensors are randomly chosen between 100 and maximum speed 150 meters per second at a random direction, and the sensors are positioned randomly between 50~100 kilometers from the target assuming an initial location with an error of 2500~5000 meters. Signal-to-noise ratio is in the range 8~10 decibels.

As an example, a stopping rule for the location mission can be set at 250 meters^2 as sample evaluated location accuracy if it can be reached within 4 updates of the sensor states, which correspond to a mission time limit of 40 seconds. Beyond the time limit, mission is aborted to avoid over exposure of the vehicles. Referring to Fig. 8, the location mission can be accomplished with or without sensor state optimization in this case. Prolonged mission, however, increases the risk of sensor loss, and thus the likelihood of mission abortion without reaching the required location accuracy. The next section discusses two ways to tolerate the effect of loss of sensors.

It is known that differential entropy measured in bits [6] of a multivariate normal distribution of $\hat{\mathbf{p}}_e$, as defined by the integrand in (27), is

$$\frac{n}{2}\log(2\pi e)+\frac{1}{2}\log det(P(\hat{\mathbf{p}}_e;\mathbf{z})),$$

which leads to a problem of minimizing

$$-\log det(G^T(\hat{\mathbf{p}}_e;\mathbf{z})C^{-1}G(\hat{\mathbf{p}}_e;\mathbf{z})), \tag{30}$$

where C is evaluated using the acquired measurement samples, and $G(\hat{\mathbf{p}}_e;\mathbf{z})$ is defined in (24). Since $\log(.)$ is monotonically increasing in its argument, minimizing (30) is equivalent to minimizing

$$det(P(\hat{\mathbf{p}}_e;\mathbf{z}))=\lambda_1(\mathbf{z})\lambda_2(\mathbf{z})\cdots\lambda_n(\mathbf{z}),$$

which in turn is equivalent to the volume minimization problem (28) because $vol(R_\kappa)$ is proportional to $\sqrt{det(P)}$. Therefore, (28) also has an entropy interpretation. For this reason, guidance under this criterion is also called an entropy-based guidance in this paper.

Although it is known that $-\log\det(X)$ is convex with respect to $X=X^T>0$ [4], $G^T(\hat{\mathbf{p}}_e;\mathbf{z})C^{-1}G(\hat{\mathbf{p}}_e;\mathbf{z})$ as a function of $\mathbf{z}$ is rather complicated. Its structure must be investigated to help find efficient and reliable algorithms to the volume minimization problem (28). We have established that when sensors are sufficiently far from the target, the volume (or entropy) minimization problem can be significantly simplified. The implicit constraints are determined by the convex subsets of reachable set A_i defined by the corresponding velocity components. Report on the simplified problem is being submitted as a separate paper. This work uses the volume-based measure $V(\hat{\mathbf{p}}_e,\mathbf{z}^+)$ as a scalar field to select sensor state update $\mathbf{z}^+$ through straightforward evaluations at a set of selected grid points.

3.2. Fault-tolerant guidance for a 4-sensor/target location mission

The effort to implement fault-tolerant guidance is described in this subsection. Rather than striving for generality, the simplest nontrivial case of a four-sensor network will be assumed. Fault-tolerance is introduced in two ways. The first way is through the guidance criterion by which sensor states are updated. The second is through the reconfiguration of the network to maximally utilize the remaining resources upon a vehicle loss. The difficulty caused by the additional cross terms in the measurement covariance due to reconfiguration is overcome by using a block diagonal upper bound [23] of the covariance in sensor state updates.

Suppose during a sensor state update, the probability of loss of a vehicle is p, and the single vehicle loss probability remains the same in subsequent intervals of updates. The probability mass function describing the number of lost vehicles in an update interval is binomial

$$w_m^l=b(l,m,p)=\binom{m}{l}p^l(1-p)^{m-l},\ l=0,\cdots,m,$$

where $m=1,2,3,4$ is assumed. Non-homogeneous probability of loss of vehicles over different airborne sensors and for different number of steps into sensor

state updates can be considered when additional information is available.

For a given m (total number of surviving vehicles), a distinct expression of guidance criterion can be written for each viable outcome of the Bernoulli trials. For example, if only one sensor survives by the time the sensor is to arrive at its updated state, the network can no longer continue its mission which requires paired sensors[5].

Denote by $\Pi_i z$ the projected sensor state to be updated resulting from the i th viable outcome upon loss of a specific set of sensors. A weighted sum of all possible viable outcomes by their respective likelihood of occurrences is now used as a fault-tolerant guidance criterion. With $m = 4$, for example, the fault-tolerant guidance criterion becomes

$$\min_{\mathbf{z}^+ \in A_c} L(\hat{\mathbf{p}}_e, \mathbf{z}^+), \tag{31}$$

where the weighted volume is given by

$$\begin{aligned} L(\hat{\mathbf{p}}_e, \mathbf{z}^+) = & V(\hat{\mathbf{p}}_e, \mathbf{z}^+) w_4^0 \\ & + \frac{1}{4}[V(\hat{\mathbf{p}}_e, \Pi_1 z^+) w_4^1 + \cdots + V(\hat{\mathbf{p}}_e, \Pi_4 z^+) w_4^1] \\ & + \frac{1}{6}]V(\hat{\mathbf{p}}_e, \Pi_5 z^+) w_4^2 + V(\hat{\mathbf{p}}_e, \Pi_6 z^+) w_4^2]. \end{aligned} \tag{32}$$

In the above expression, the 6 volumes of the 6 viable outcomes from which the network survives, except for the first, are obtained from the 2-sensor network. Each volume is associated with a network of a specific configuration, and each involves a distinct approximate Fisher information matrix [13] at the current estimate $\hat{\mathbf{p}}_e$

$$P^{-1}(\hat{\mathbf{p}}_e, \Pi_i z^+) = G^T(\hat{\mathbf{p}}_e, \Pi_i z^+) C_{\Pi_i}^{-1} G(\hat{\mathbf{p}}_e, \Pi_i z^+). \tag{33}$$

C_{Π_i} must be evaluated from the available measurement samples for each configuration. Fig. 10 shows a more pronounced benefit of using the fault-tolerant guidance criterion (32) as the likelihood of vehicle loss increases. The vertical axis is the ratio of the area of the concentration ellipse at 50% chance of hit at $\mathbf{z}^+$ using the knowledge on vehicle loss to that ignoring the knowledge for each of the six vehicle loss probabilities, where $50\% = Pr[\hat{\mathbf{p}}_e^+ \in R_{\kappa=\log 4}]$. The covariance based on which concentration $R_{\kappa=\log 4}$, as defined in (26), is evaluated by sample

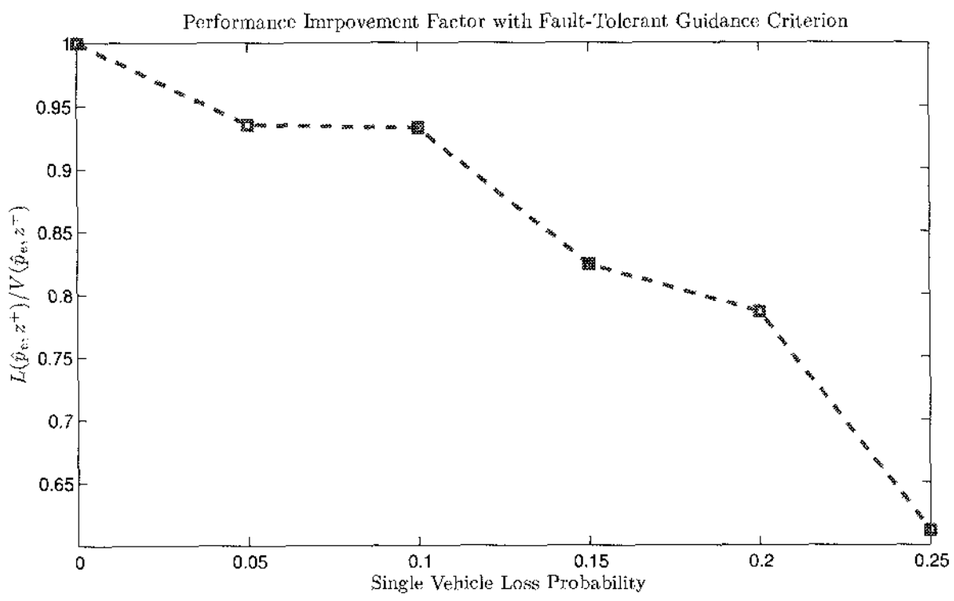

Fig. 10. Ratio of volumes of concentration ellipses with and without fault-tolerant considerations as a function of vehicle loss probability.

covariance formed from the 150 independent location estimates.

Fault-tolerance can be further enhanced by reconfiguration of the network architecture through pairing the single surviving sensor of the faulty pair with one of the sensors of the healthy pair, or through pairing the two single surviving sensors from the two faulty pairs. Reconfiguration requires that terms in (32) be modified.

With the $2N$ sensors exclusively paired, $C = diag\{C_1, C_2, \cdots, C_N\}$. Each 2×2 diagonal block C_i can be estimated from the collected samples using, for example, short time Fourier transform [8]. Forming two pairs with three independent sensors triggers the need to calculate additional cross terms in the measurement covariance matrix C_{Π_i}, for which no reliable means of calculation is yet available. To avoid the need to calculate additional cross terms in the measurement covariance matrix, C_{Π_i} is replaced by a block diagonal upper bound [23]

$$C_{\Pi_i} \le \begin{bmatrix} \eta_1 C_{\Pi_i,1} & 0_2 \\ 0_2 & \eta\ C_{\ i,} \end{bmatrix} \equiv \bar{C}_{\Pi_i}, \tag{34}$$

where

$$\eta_j = \frac{\sqrt{\xi_1 C_{\Pi_i,1} \xi_1} + \sqrt{\xi_2 C_{\Pi_i,2} \xi_2}}{\sqrt{\xi_j C_{\Pi_i,j} \xi_j}},\ \xi_j \neq 0,\ j = 1,2. \tag{35}$$

Note that the upper bound involves calculations of only the original 2×2 diagonal blocks of C_{Π_i} for which the short time Fourier transform method can be used.

Let $\bar{V}$ and $\bar{L}$ denote the volume and the weighted sum of volumes, respectively, resulting from replacing C_{Π_i} by $\bar{C}_{\Pi_i}$ in (32). It is now shown

[5] Mission abortion condition can be relaxed to exclude that of a single surviving sensor in which case the sensing mechanism must be switched to that of a single platform [24] with much reduced data acquisition quality and speed.

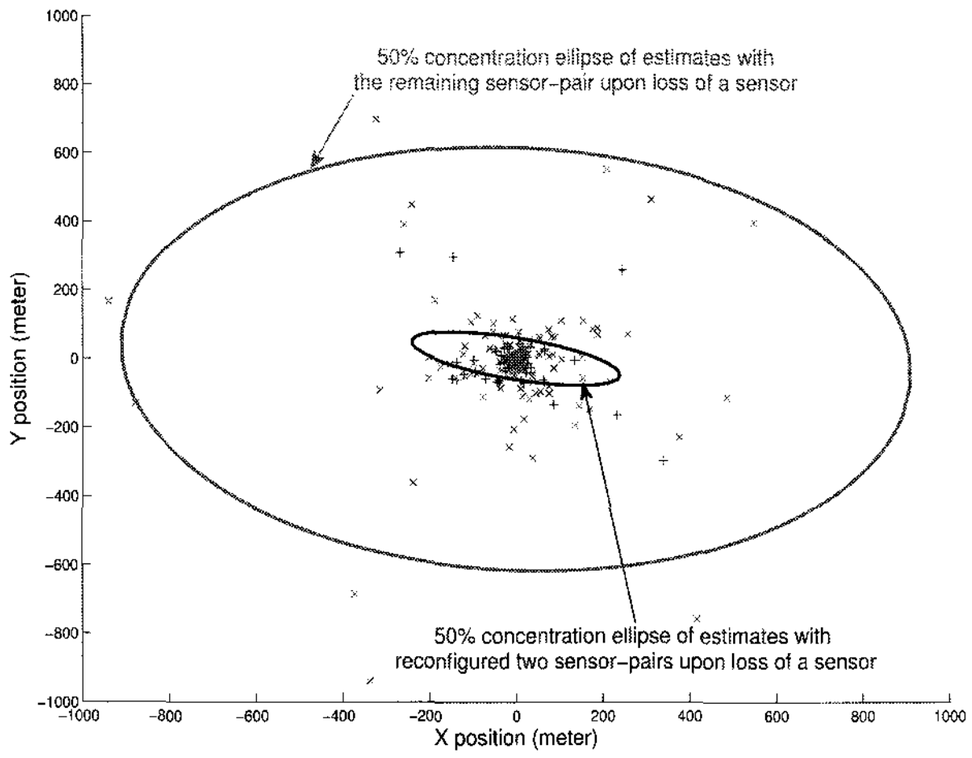

Fig. 11. Benefit of network reconfiguration shown through comparison of the estimates (magenta) from the remaining 1 sensor-pair with the estimates (blue) of reconfigured 2 sensor-pairs in case of loss of a sensor.

that $\min_{\mathbf{z}^+ \in A_c} \bar{L}(\hat{\mathbf{p}}_e, \mathbf{z}^+)$ bounds $\min_{\mathbf{z}^+ \in A_c} L(\hat{\mathbf{p}}_e, \mathbf{z}^+)$ from above. Let $\bar{\mathbf{z}}^+ \in A_c$ minimizes $\bar{L}(\hat{\mathbf{p}}_e, \mathbf{z}^+)$, and $\tilde{\mathbf{z}}^+ \in A_c$ minimizes $L(\hat{\mathbf{p}}_e, \mathbf{z}^+)$. Then

$$\bar{L}(\hat{\mathbf{p}}_e, \bar{\mathbf{z}}^+) - L(\hat{\mathbf{p}}_e, \tilde{\mathbf{z}}^+) \geq \bar{L}(\hat{\mathbf{p}}_e, \bar{\mathbf{z}}^+) - L(\hat{\mathbf{p}}_e, \bar{\mathbf{z}}^+)$$
$$= \frac{1}{4} w_4^1 \sum_{i=1}^{4} [\bar{V}(\hat{\mathbf{p}}_e, \Pi_i \bar{\mathbf{z}}^+) - V(\hat{\mathbf{p}}_e, \Pi_i \bar{\mathbf{z}}^+)]. \quad (36)$$

(25) implies that $\bar{P}_{\Pi_i} \equiv [G^T \bar{C}_{\Pi_i}^{-1} G]^{-1} \geq P_{\Pi_i}$ whenever $\bar{C}_{\Pi_i} \geq C_{\Pi_i}$. From the definition of the volume of an ellipsoid given by (26) and (28), $\bar{V}(\hat{\mathbf{p}}_e, \Pi_i \bar{\mathbf{z}}^+) \geq V(\hat{\mathbf{p}}_e, \Pi_i \bar{\mathbf{z}}^+)$. Therefore, the right most quantity in (36) is nonnegative, and the conclusion follows.

Fig. 11 shows the significant advantage with network reconfiguration in case of a sensor loss, despite the upper bound used in calculating C_{Π_i}. The 50% concentration ellipses are drawn based on the location estimates of 150 independent replications with approximately 15 decibels of the signal to noise ratio in received microwave signals. The single sensor loss probability during an update period is assumed at 0.05. It is noted that the 50% concentration ellipse is calculated assuming that the sample covariance used for this purpose is that of a normal distribution. With only 150 sample estimates, however, the sample distribution can be far from normal, and therefore the probability that an estimate resides in R_{ln4} can be very different from 50%. Nevertheless, the volume of R_{ln4} provides a good measure for comparison of accuracy.

4. CONCLUSIONS

This paper sought to determine supervisory control policies that best configure an airborne location sensor network to provide a high degree of guarantee of prompt completion of coordinated data acquisition and processing missions in the face of loss of vehicles. Use of redundancy, dynamic allocation of participating sensors, sensing principle-based guidance, and network reconfiguration were the key enablers.

The paper presented a queuing network approach to optimal sensor-pair assignment to locate detected targets for a small scale airborne sensor network, where use of redundancy is balanced with avoiding more vehicle exposure. The paper also introduced fault-tolerant concept into generating vehicle trajectories that are optimized to facilitate acquired data quality. The paper demonstrated significant sensing performance improvement through implementing fault-tolerant tasking and fault-tolerant guidance.

A number of related issues are being investigated. In addition to loss of sensors, degradation of network performance can also be the result of broken communication links. Such incidents are modeled as intermittent faults of the servers in queuing networks. The effects of such faults will be studied using discrete event simulations, which will also examine possible emergent phenomenon of larger networks, and non-homogeneous sensors and targets.

On the guidance side, efficient vehicle state optimization remains open, algorithms for determining the reachable sets for the vehicles are being developed. A candidate approach to coordinated control of vehicles for synchronous data acquisition has been identified [11].

REFERENCES

[1] P. Antsaklis and J. Baillieul, editors, "Special issue on technology of networked control systems," *Proc. of the IEEE*, vol. 95, no. 1, 2007.

[2] R. W. Beard, T. W. McLain, M. A. Goodrich, and E. P. Anderson, "Coordinated target assignment and intercept for unmanned air vehicles," *IEEE Trans. on Robotics and Automation*, vol. 18, pp. 911-922, 2002.

[3] D. P. Bertsekas, *Dynamic Programming and Optimal Control*, Volume 1 & Volume 2, Athena Scientific, 1995.

[4] S. P. Boyd and L. Vandenberghe, *Convex Optimization*, Cambridge University Press, 2004.

[5] C. G. Cassandras and S. Lafortune, *Introduction to Discrete Event Systems*, Kluwer, 1999.

[6] T. M. Cover and J. A. Thomas, *Elements of Information Theory*, John Wiley & Sons, 1991.

[7] J. E. Dennis, *Nonlinear Least Squares, State of*

Art in Numerical Analysis, ed. D. Jacobs, Academic Press, 1977.

[8] M. L. Fowler and M. Chen, "Evaluating Fisher information from data for task-driven data compression," *Proceedings of Conference on Information Sciences and Systems*, 2005.

[9] K. C. Ho and Y. T. Chan, "Geolocation of a known altitude object from TDOA and FDOA measurements," *IEEE Trans. on Aerospace and Electronic Systems*, vol. 33, pp. 770-782, 1997.

[10] K. C. Ho and W. Xu, "An accurate algebraic solution for moving source location using TDOA and FDOA measurements," *IEEE Trans. on Signal Processing*, vol. 52, pp. 2453-2463, 2004.

[11] I. Kaminer, O. Yakimenko, A. Pascoal, and R. Ghabcheloo, "Path generation, path following and coordinated control for time-critical missions of multiple UAVs," *Proc. of American Control Conference*, 2006.

[12] E. P. C. Kao, *An Introduction to Stochastic Processes*, Duxbury Press, 1997.

[13] S. M. Kay, *Fundamentals of Statistical Signal Processing: Estimation Theory*, Prentice Hall, 1988.

[14] G. Klir, and M. Wierman, *Uncertainty-Based Information: Elements of Generalized Information Theory,* Second Edition, Physica-Verlag/Springer Verlag, 1999.

[15] MathWorks, *Optimization Toolbox User's Guide, For Use with MATLAB, Version 3*, The MathWorks, Inc., 2006.

[16] MathWorks, *SimEvents User's Guide, For Use with Simulink*, The MathWorks, Inc., 2006.

[17] S. Oh, L. Scheanto, P. Chen, and S. Sastry, "Tracking and coordination of multiple agents using sensor networks: System design, algorithms, and experiments," *Proc. of the IEEE*, vol. 95, pp. 234-254, 2007.

[18] R. A. Poisel, *Electronic Warfare Target Location Methods*, Artech House, 2005.

[19] T. Samad, J. S. Bay, and D. Godbole, "Network-centric systems for military operations in urban terrain: the role of UAVs," *Proc. of the IEEE*, vol. 95, pp. 92-107, 2007.

[20] D. J. Torrieri, "Statistical theory of passive location systems," *IEEE Trans. on Aerospace and Electronic Systems,* vol. 20, pp. 183-198, 1983.

[21] M. Valenti, B. Bethke, J. P. How, D. P. Farias, and J. Vian, "Embedding health management into mission tasking for UAV teams," *Proc. American Control Conference*, 2007.

[22] N. E. Wu, M. C. Ruschmann, and M. H. Linderman, "Fault-tolerant control of a distributed database system," *Journal of Control Science of Engineering, Special Issue, Robustness Issues in Fault Diagnosis and Fault Tolerant Control*, Jakob Stoustrup, and Kemin Zhou, Guest Editors, Article ID 310652, 2008.

[23] N. E. Wu and M. L. Fowler, "An Error bound for sensor fusion with application to Doppler frequency based emitter location," *IEEE Trans. on Automatic Control*, vol. 51, pp. 631-635, 2006.

[24] N. E. Wu and M. L. Fowler, "Aperture error mitigation via local-state estimation for frequency-based emitter location," *IEEE Trans. on Aerospace and Electronics*, vol. 39, pp. 414-428, 2003.

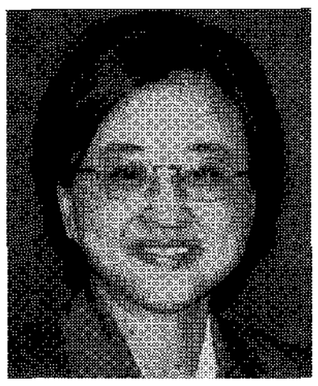

N. Eva Wu received her BSEE degree from Northwestern Telecommunication Engineering Institute, China in 1982, and MSEE and Ph.D. degrees from University of Minnesota in 1983, and 1987 respectively. She is currently a Professor in the Department of Electrical and Computer Engineering at Binghamton University, SUNY.

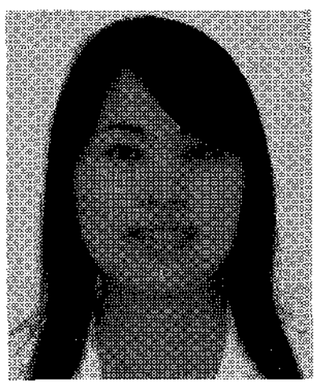

Yan Guo received her BSEE degree from Clarkson University in 2004 and MSEE degree from Binghamton University in 2007.

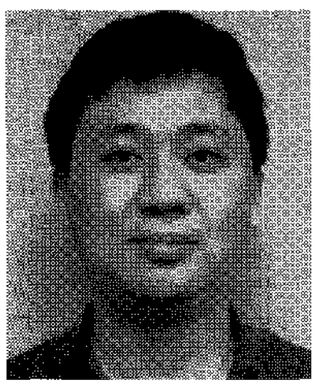

Kun Huang received his BSEE degree from Xi'an Jiaotong University in 1996 and MSCS degree from University at Buffalo in 2002. He is currently enrolled as a Ph.D. candidate at Binghamton University.

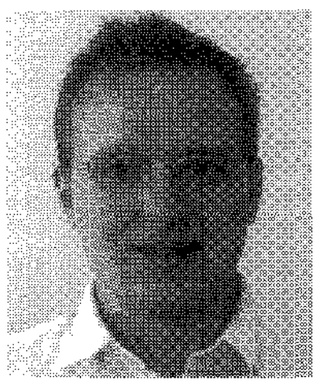

Matthew C. Ruschmann received his BSEE degree from Clarkson University in 2003 and MSEE degree from Binghamton University in 2006. He is currently a Ph.D. candidate enrolled at Binghamton University.

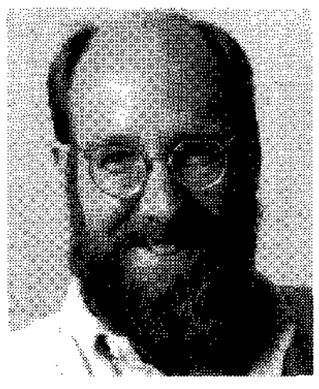

Mark L. Fowler received the B.T. in Electrical Engineering Technology from SUNY at Binghamton in 1984 and the Ph.D. in Electrical Engineering from Pennsylvania State University in 1991. Since 1999 he has been in the Department of Electrical and Computer Engineering at Binghamton University, where he is currently a Professor.